Electrostatic Interactions Regulate Desensitization of the Nicotinic Acetylcholine Receptor

Xing-Zhi Song and Steen E. Pedersen
Department of Molecular Physiology and Biophysics, Baylor College of Medicine, Houston, Texas 77030 USA

ABSTRACT To determine the importance of electrostatic interactions for agonist binding to the nicotinic acetylcholine receptor (AChR), we examined the affinity of the fluorescent agonist dansyl-C6-choline for the AChR. Increasing ionic strength decreased the binding affinity in a noncompetitive manner and increased the Hill coefficient of binding. Small cations did not compete directly for dansyl-C6-choline binding. The sensitivity to ionic strength was reduced in the presence of proadifen, a noncompetitive antagonist that desensitizes the receptor. Moreover, at low ionic strength, the dansyl-C6-choline affinities were similar in the absence or presence of proadifen, a result consistent with the receptor being desensitized at low ionic strength. Similar ionic strength effects were observed for the binding of the noncompetitive antagonist [^{3}H]ethidium when examined in the presence and absence of agonist to desensitize the AChR. Therefore, ionic strength modulates binding affinity through at least two mechanisms: by influencing the conformation of the AChR and by electrostatic effects at the binding sites. The results show that charge-charge interactions regulate the desensitization of the receptor. Analysis of dansyl-C6-choline binding to the desensitized conformation using the Debye-Hückel equation was consistent with the presence of five to nine negative charges within 20 Å of the acetylcholine binding sites.

INTRODUCTION

The nicotinic acetylcholine receptor (AChR) is a cation-selective, ligand-gated ion channel found at the vertebrate neuromuscular junction and in the electric organ of *Torpedo californica*. It is a transmembrane pentamer composed of four different subunits assembled with a stoichiometry $\alpha_2\beta\gamma\delta$ around an axis of pseudosymmetry perpendicular to the plane of the membrane (Barrantes, 1998; Devillers-Thiery et al., 1993; Hucho et al., 1996). The AChR pentamer contains two activating binding sites for acetylcholine (ACh); one site is at the interface between the first α subunit and the γ subunit, and the second site is between the second α subunit and the δ subunit (Blount and Merlie, 1989; Pedersen and Cohen, 1990). The binding of two agonist molecules to the ACh sites induces the channel to open. Prolonged exposure to agonist results in the desensitization of the receptor into a nonconductive state. The AChR also contains a high affinity binding site for noncompetitive antagonists (NCA); the site is within the ion channel, which is located at the axis of the pseudosymmetry in the transmembrane region. NCAs appear to inhibit channel activity by steric block of ion flux (Neher and Steinbach, 1978).

At physiological conditions the AChR exists in equilibrium between the resting conformation and the desensitized conformation. Because the conformational state of the AChR influences ligand binding, binding of agonists to ACh sites or NCAs to the channel site can be modeled by cyclic schemes (Schemes I and II) as shown below (Katz and Thesleff, 1957; Ochoa et al., 1989). Scheme I shows a single binding site, which describes the binding of NCAs. For ligands that bind two sites, such as agonists, a similar scheme (II) with two binding steps applies. K_R and K_D represent the microscopic dissociation constants for the resting and desensitized conformations, respectively; M is the allosteric constant, which equals the ratio of concentrations of desensitized to resting AChR in the absence of ligand (L).

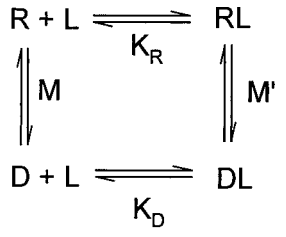

Scheme I

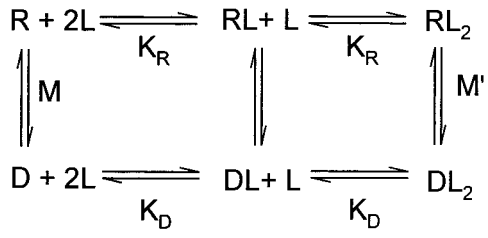

Scheme II

The conformational equilibrium is regulated by binding of agonists and by the binding of NCAs (Ochoa et al., 1989). NCAs may influence the conformation of the AChR by

Received for publication 23 September 1999 and in final form 29 November 1999.

Address reprint requests to Steen E. Pedersen, Department of Molecular Physiology and Biophysics, Baylor College of Medicine, One Baylor Plaza, Houston, TX 77030. Tel.: 713-798-3888; Fax: 713-798-3475; E-mail: pedersen@bcm.tmc.edu.

0006-3495/00/03/1324/11 $2.00

stabilizing either the resting or the desensitized conformation, depending on the exact ligand. For example, proadifen, phencyclidine, and ethidium bromide (EB) significantly increase agonist affinity because they promote the desensitized conformation (Cohen et al., 1986; Krodel et al., 1979). Reciprocally, the presence of an agonist such as acetylcholine or carbamylcholine (Carb) increases the binding affinity of desensitizing NCAs for the channel site (Changeux et al., 1984; Walker et al., 1982).

The positively charged character of agonists and competitive antagonists suggests that electrostatic interactions may play an important role for ligand binding and the receptor's function; at low ionic strength the binding affinity of *d*-tubocurarine to AChR is stronger (Neubig and Cohen, 1979) and the rate of α-bungarotoxin binding increases dramatically (Schmidt and Raftery, 1974). However, various labeling studies have identified primarily aromatic amino acid residues that contribute to ACh binding, including the following residues in the α-subunit: αTyr-93, αTrp-149, αTyr-190, and αTyr-198 (Devillers-Thiery et al., 1993). The role of these residues in binding is consistent with the hypothesis that the cationic moiety associated with cholinergic ligands is stabilized predominantly by interactions with aromatic ring π-electrons (Dougherty, 1996; Zhong et al., 1998).

Stabilization of the cation by formation of a charge pair or through electrostatic interactions, however, has not been excluded. A substantial electrical potential (-80 mV) was found by the relative reactivity of variously charged methanethiosulfonate derivatives with αCys-192/193, suggesting the presence of several negative charges near the binding sites (Stauffer and Karlin, 1994). In contrast, power saturation EPR of spin-labeled ligands yielded a smaller electrostatic potential of -15 mV (Addona et al., 1997). Several candidate negative charges that affect binding were determined by cross-linking studies (δAsp-180 (Czajkowski and Karlin, 1995; Martin et al., 1996)) and site-directed mutagenesis (αAsp-152 (Sugiyama et al., 1996)). These residues may constitute a counter-charge or provide electrostatic stabilization for the cholinergic cation.

Despite the substantial data supporting a mechanism of binding that included electrostatic attraction, it remains unclear whether such stabilization occurs by salt-bridge formation, long-range attraction, or both. The increasing evidence for aromatic π-electron stabilization of the organic cation does not exclude the presence of electrostatic stabilization (e.g., see Tan et al., 1993). Nonetheless, the number of charged groups and their distribution near the ACh sites is not known, nor has any relevance of electrostatic interactions to binding at physiological ionic strength been clearly demonstrated.

In the present study we measured the ionic strength dependence of the binding affinity of a fluorescent analog of acetylcholine dansyl-C6-choline (Dns-C6-Cho) (Heidmann et al., 1983) to determine the significance of electrostatic interactions. The data suggest a broad distribution of five to nine negative charges near the agonist binding sites. In addition, we found that the AChR is relatively desensitized at low ionic strength; at high ionic strength the resting state is relatively stabilized. A similar conclusion was reached by examining the ionic strength dependence of the affinity of [^{3}H]EB, an NCA. The ionic strength effect on the conformational equilibrium found by both agonist and NCA binding suggests that charge-charge interactions regulate the desensitization of the receptor.

MATERIALS AND METHODS

Materials

EB, carbamylcholine chloride (Carb), sodium dodecyl sulfate (SDS), dansyl chloride, and phencyclidine hydrochloride (PCP) were purchased from Sigma Chemical Co. (St. Louis, MO); proadifen was from Research Biochemicals International (Natick, MA); Hepes was from Boehringer-Mannheim (Indianapolis, IN); NaCl, LiCl, and KCl were from Fisher Science (Pittsburgh, PA); RbCl was from EM Science (Gibbstown, NJ); and CsCl was from Amresco (Solon, OH).

AChR-rich membranes were isolated from *Torpedo californica* electric organ (Marinus Inc., Long Beach, CA or Aquatic Research Consultants, San Pedro, CA) by differential sucrose ultracentrifugation as described previously (Pedersen et al., 1986; Sobel et al., 1977). Purified membranes typically contained 1–2 nmol of ACh sites/mg of protein as measured by binding of [^{3}H]ACh (Pedersen, 1995). Membranes were stored in 37% sucrose/0.02% NaN_3 at -80°C under argon. The AChR-rich membranes were treated with diisopropylfluorophosphonate (Aldrich Chemical Co., Milwaukee, WI) to inactivate acetylcholinesterase immediately before binding experiments with Dns-C6-Cho.

Dns-C6-Cho was synthesized from dansyl chloride and N-carbobenzoxy-ϵ-aminocaproic acid (Bachem, King of Prussia, PA) using the procedures in the literature (Waksman et al., 1976). [^{3}H]EB (1.15 Ci/mmol) was obtained as described previously (Lurtz et al., 1997).

Dns-C6-Cho fluorescence binding assays

The interaction of Dns-C6-Cho with the AChR-rich membranes was monitored under conditions of energy transfer from protein tryptophan(s), which results in an ~10-fold increase in fluorescence intensity at the maximal emission wavelength (λ_{em} = 557 nm) (Waksman et al., 1976). Fluorescence data were collected on an SLM 8000C fluorometer. The excitation light from a 350 W xenon short arc lamp was filtered with a UV pass filter (Oriel 59152). Each sample was excited at 292 nm with a 2.0 nm bandwidth. To improve the signal, the emission light was collected directly by mounting the photomultiplier on the emission window without going through the monochromator and was only filtered through a 495-nm cut-on filter (Oriel 59492).

Dns-C6-Cho binding assays were carried out in 20 mM Hepes (pH = 7.0) at various ionic strengths that were controlled by the NaCl concentration. Binding isotherms were measured by titration of AChR-rich membrane suspensions with a concentrated Dns-C6-Cho solution. Excess Carb (1 mM) was used to define the nonspecific fluorescence of Dns-C6-Cho in samples titrated in parallel. Binding measurements in the presence of proadifen were also carried out in parallel. To observe the effects of salt in more detail we chose one set of concentrations of Dns-C6-Cho and AChR that were kept constant, and assayed separate samples that contained varying salt concentrations (NaCl, LiCl, KCl, RbCl, and CsCl) by measuring fluorescence of Dns-C6-Cho, as described above.

[^{3}H]EB binding assays

[^{3}H]EB binding assays were performed by centrifugation as described previously (Pedersen, 1995). Both bound and free [^{3}H]EB were measured by counting the pellet and supernatant for each sample. To observe the effect of ionic strength on EB binding over a broad range we picked a single concentration of [^{3}H]EB and AChR, and varied the concentration of NaCl. Nonspecific binding was determined by including excess of the inhibitor PCP (0.5 mM).

Binding data analysis

To define the dissociation constant, K, and the Hill coefficient, n, Dns-C6-Cho binding isotherms were fitted with the Hill equation (Eq. 1) by nonlinear regression (SigmaPlot vs. 2, Jandel Scientific).

$$F_L = \frac{C \cdot R_0}{1 + (K/[L])^n} \tag{1}$$

where $[L]$ is the Dns-C6-Cho concentration, F_L is the fluorescence intensity after subtraction of the corresponding nonspecific binding, R_0 is the total binding site concentration, and C is the proportionality constant of the fluorescence intensity to bound ligand concentration ($F_L = C \cdot [RL]$). C was determined as a freely fit parameter in the nonlinear regression and was obtained simultaneously with K and n. In cases where the observed Hill coefficient n was near 1, as in the presence of proadifen, the binding data were sometimes fit with the simple binding equation (i.e., Eq. 1 with $n = 1$).

The data were usually analyzed in terms of the total Dns-C6-Cho concentration added. In some cases the free Dns-C6-Cho differed substantially from the added concentration because of binding to the AChR, particularly in the cases of high-affinity binding at low ionic strength or in the presence of proadifen. To avoid error in the determination of the K value, such data were fit with Eq. 2, which explicitly accounts for bound ligand. L_0 is the total ligand concentration added.

$$F_L = \frac{C}{2}\left(K + R_0 + L_0 - \sqrt{(K + R_0 + L_0)^2 - 4R_0L_0}\right) \tag{2}$$

Eq. 2 was used only in situations where the Hill coefficient was 1. This improved the accuracy for the determination of K at conditions of high affinity. In no case did the values determined by Eqs. 1 and 2 differ by more than twofold, and usually <20%.

The binding data obtained at single concentrations of Dns-C6-Cho and AChR were analyzed to calculate the dissociation constants using Eq. 3, which was derived from the Hill equation:

$$K = \left(\frac{C \cdot R_0}{F_L} - 1\right)^{1/n} \cdot \left(L_0 - \frac{F_L}{C}\right) \tag{3}$$

For these experiments, C was experimentally determined from a calibration curve of bound Dns-C6-Cho fluorescence versus Dns-C6-Cho concentration. The calibration curve was measured with a large excess of AChR over Dns-C6-Cho under conditions where nearly all the Dns-C6-Cho was bound to the receptor.

The dissociation constant of [^{3}H]EB was calculated using the following equation:

$$K = (R_0 - L_B)(L_F/L_B) \tag{4}$$

where R_0 is the total AChR concentration and L_F and L_B are the concentrations of free ligand and specific bound ligand, respectively; these values were obtained by scintillation counting of bound and free [^{3}H]EB.

Effective charges at the binding site

To calculate the effective charges at the binding sites the ionic strength dependence of the dissociation constant could be fitted with an equation derived from the Debye-Hückel theory (Nolte et al., 1980). The Debye-Hückel limiting law treats the charged species (i) as a point charge (z_ie) and gives the activity coefficient (γ_i) as a function of ionic strength (I) in a dilute solution:

$$\log \gamma_i = -A \cdot z_i^2 \cdot \sqrt{I} \tag{5}$$

Considering the size of the charged species, the Debye-Hückel equation can be modified to include the effective radius of the charge (r) (Levine, 1988, pp. 281–283):

$$\log \gamma_i = -\frac{A \cdot z_i^2 \cdot \sqrt{I}}{1 + r \cdot B \cdot \sqrt{I}} \tag{6}$$

where A and B are thermodynamic constants ($A = 0.509$, $B = 3.291\ \mathrm{nm}^{-1} \cdot \mathrm{M}^{-1/2}$ at 298 K in water). For a binding reaction between two charged species, R (with a charge z_R) and L (with a charge z_L), the thermodynamic dissociation constant K_0 depends on the activity, a_i, of each species:

$$K_0 = \frac{a_R \cdot a_L}{a_{RL}} = \frac{[R] \cdot [L]}{[RL]} \cdot \frac{\gamma_R \cdot \gamma_L}{\gamma_{RL}} = K \cdot \frac{\gamma_R \cdot \gamma_L}{\gamma_{RL}} \tag{7}$$

The charge of RL, z_{RL}, equals $z_R + z_L$; further substituting Eq. 6 into Eq. 7, the dependence of the concentration dissociation constant K on ionic strength is given by Eq. 8:

$$\log K = \log K_0 - \frac{2 \cdot A \cdot z_R \cdot z_L \cdot \sqrt{I}}{1 + r \cdot B \cdot \sqrt{I}} \tag{8}$$

Assuming the known ligand charge (z_L), the effective receptor charge, z_R, and the charge distribution, r, can be obtained by fitting data of dissociation constant versus ionic strength with Eq. 8. Nolte et al. (1980) used this equation to analyze the effective charge distribution near the reactive site of acetylcholinesterase.

Determination of the allosteric constant, *M*

Under the cyclic scheme of single site binding shown in the introduction (Scheme I), the fractional occupancy of the binding sites (Y) can be expressed in terms of the microscopic dissociation constants for the resting state (K_R) and for the desensitized state (K_D), and M.

$$Y = \frac{[RL] + [DL]}{[R] + [RL] + [D] + [DL]} = \frac{\frac{[L]}{K_R} + M \cdot \frac{[L]}{K_D}}{1 + \frac{[L]}{K_R} + M + M \cdot \frac{[L]}{K_D}} \tag{9}$$

When 50% of the sites are bound with ligand ($Y = 0.5$), the ligand concentration $[L]$ equals the apparent dissociation constant (K_{app}). From Eq. 9, M is given by Eq. 10:

$$M = \frac{K_D \cdot (K_R - K_{app})}{K_R \cdot (K_{app} - K_D)} \tag{10}$$

$$M \approx \frac{K_D}{K_{app} - K_D} \tag{11}$$

When $K_R \gg K_D$ and $K_R \gg K_{app}$, M is closely approximated by Eq. 11. This approximation is generally valid for cholinergic ligands that bind with substantially lower affinity to the native resting state (e.g., $K_R \sim 5$–$500\ \mu M$ for acetylcholine (Sine et al., 1990)). K_{app} and K_D are measured in the absence and presence of a desensitizing allosteric ligand, respectively. For ligand binding to two sites with equal affinity, as in Scheme II ($K_{R1} = K_{R2} = K_R$ for the R-state, $K_{D1} = K_{D2} = K_D$ for the D-state), the expression for M can be similarly derived.

$$M = \frac{K_{D1} \cdot K_{D2} \cdot (K_{R1} \cdot K_{R2} - K_{app}^2)}{K_{R1} \cdot K_{R2} \cdot (K_{app}^2 - K_{D1} \cdot K_{D2})}$$

$$= \frac{K_D^2 \cdot (K_R^2 - K_{app}^2)}{K_R^2 \cdot (K_{app}^2 - K_D^2)} \approx \frac{K_D^2}{K_{app}^2 - K_D^2} \qquad (12)$$

RESULTS

To determine the importance of ionic interactions for agonist binding to the AChR we examined the binding of the fluorescent agonist Dns-C6-Cho at various ionic strengths. In preliminary experiments we had observed that Dns-C6-Cho binding was enhanced at low ionic strength and was no longer affected by the presence of a desensitizing NCA. Because the conformational state of the AChR will influence agonist binding, it was necessary to distinguish the relative influence of ionic strength changes on the conformational equilibrium versus pure ionic interactions on the binding of Dns-C6-Cho.

Proadifen fails to modulate agonist binding at low ionic strength

Proadifen desensitizes the receptor by binding to the high-affinity NCA site of the AChR (Krodel et al., 1979). The extent of desensitization was observed by changes in affinity of Dns-C6-Cho, as monitored by changes in fluorescence intensity. We measured the change in Dns-C6-Cho binding to the AChR upon titration with increasing concentrations of proadifen at different NaCl concentrations. Shown in Fig. 1 are the data at 0, 50, and 250 mM NaCl. The lower curve (▲) shows the effect of proadifen in 250 mM NaCl, which is near the physiological salt concentration; the fluorescence intensity of bound Dns-C6-Cho increases with proadifen at concentrations near 2 μM. The increase can be fit to a simple, single-site binding equation, indicating that the desensitization and the increased binding affinity of Dns-C6-Cho are caused by the noncompetitive binding of proadifen. At higher concentrations ($\sim$100 μM), proadifen decreases the Dns-C6-Cho binding, an effect likely due to direct, competitive binding to the ACh sites.

At low ionic strength ([NaCl] = 0), Dns-C6-Cho affinity was much higher, as observed by the stronger fluorescent signal (●). The fluorescence was unaffected by proadifen until concentrations that decrease binding were reached at $>$10 μM. In 50 mM NaCl the effects were intermediate; the affinity increase due to proadifen was smaller and occurred at lower concentrations than in 250 mM NaCl. The intrinsic affinity of proadifen appeared to increase at lower ionic strength, whereas the allosteric effect on agonist binding was gradually lost: an increase in potency and a loss of efficacy. The curves also indicated the optimum concentrations of proadifen for later experiments that provide maximal increase in agonist binding without interference from binding to the ACh sites (i.e., 1–10 μM).

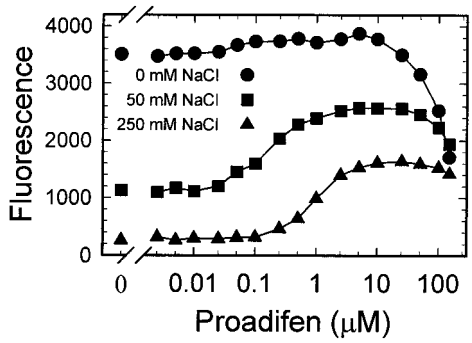

FIGURE 1 The proadifen dependence of specifically bound Dns-C6-Cho fluorescence at various ionic strengths. AChR-rich membranes (5 nM ACh sites) were incubated with Dns-C6-Cho (6 nM) in 20 mM Hepes (pH 7.0) plus NaCl (●, 0 mM; ■, 50 mM; ▲, 250 mM) and the indicated concentrations of proadifen for 1 h. Fluorescence measurements were carried out as described in Materials and Methods. The plots show specific fluorescence, the difference between binding in the presence and absence of 1 mM carbamylcholine.

Dns-C6-Cho affinity measured by binding isotherms

Binding isotherms of Dns-C6-Cho were measured at various concentrations of NaCl by titration of AChR with Dns-C6-Cho in the absence and presence of proadifen. The typical isotherms of specific binding at 0 mM and 250 mM NaCl are displayed in Fig. 2. Panel *A* shows binding of Dns-C6-Cho to AChR-rich vesicles at 250 mM NaCl, near physiological ionic strength. The solid circles show sigmoid binding that was fit to the Hill equation (Eq. 1), as indicated by the curves. In the presence of proadifen the data displayed hyperbolic concentration dependence that was well fit by the simple binding equation (Eq. 1 with $n = 1$). The K_{app} was decreased relative to binding in the absence of proadifen with apparent loss of cooperativity, an observation consistent with proadifen increasing binding affinity by desensitizing the AChR. In contrast, at low ionic strength (Fig. 2 *B*), binding was similar in affinity and noncooperative, regardless of the presence of proadifen. The inset in Fig. 2 shows the original total and nonspecific fluorescence data that correspond to the solid circles in Fig. 2 *B*.

To determine the NaCl concentration range that affects Dns-C6-Cho affinity, binding isotherms were determined in the same manner as described in Fig. 2, with NaCl concentrations that varied from 0 to 1 M. The data were fitted with

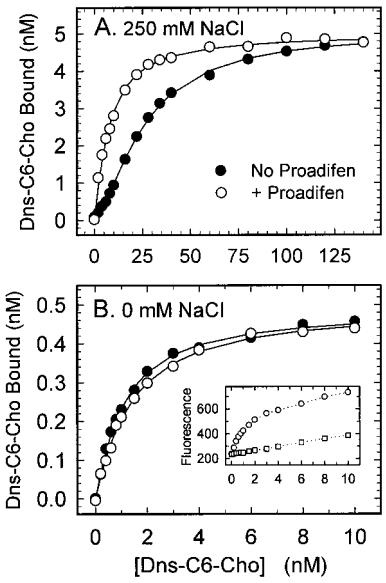

FIGURE 2 Dns-C6-Cho binding to the AChR in low and high ionic strength. (A) AChR-rich vesicles (5 nM ACh sites) were incubated in 20 mM Hepes/250 mM NaCl in the presence or absence of 1 mM Carb. Fluorescence was measured while titrating the vesicle suspension with Dns-C6-Cho, as described in Materials and Methods. Specific binding was determined by subtraction of data obtained in the presence of Carb. The specific binding is shown for data obtained in the absence (●) or presence (○) of 10 μM proadifen. (*B*) AChR-rich vesicles (0.5 nM ACh sites) were titrated in 20 mM Hepes and the binding isotherms determined as described for (*A*). For both panels, the specific fluorescence intensity was normalized to the ACh site concentrations and the data fitted with the Hill equation (*solid curves*). The inset in (*B*) shows the uncorrected fluorescence titration data obtained in the absence (○) and presence (□) of 1 mM Carb in 20 mM Hepes. The following K_{app} values were determined for the presence and absence of proadifen, respectively: (*A*) K = 7.9 nM (n = 1.1) and 27 nM (n = 1.6); (*B*) K = 1.35 nM (n = 1.1) and 1.27 nM (n = 1.1).

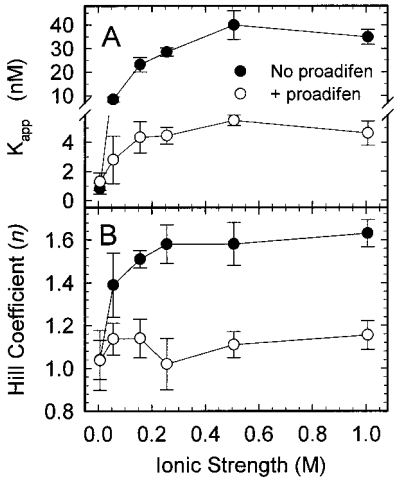

FIGURE 3 The K_{app} and the Hill coefficient of Dns-C6-Cho binding are affected by ionic strength. Dns-C6-Cho binding isotherms were measured by titration of Dns-C6-Cho into an AChR-rich membrane suspension, as described in Fig. 2 and in Materials and Methods. AChR-rich membranes (0.5 nM at [NaCl] = 0 mM; 1 or 5 nM at [NaCl] = 50 mM; 5 nM at higher ionic strengths) were pre-incubated with indicated concentrations of NaCl without proadifen (●) or with proadifen (○, 1 μM at 0 mM NaCl, 10 μM for all others) in 20 mM Hepes (pH 7.0) for 1 h. Titrations were carried out by addition of concentrated Dns-C6-Cho solutions; nonspecific binding was determined in parallel titrations carried out in the presence of 1 mM Carb. After subtraction of nonspecific binding, the data were fit to the Hill equation, Eq. 1. (*A*) Dissociation constant, K_{app}, and (*B*) Hill coefficient. Error bars are the standard deviations of 4–20 independent determinations.

the Hill equation to calculate the dissociation constant, K_{app}, and Hill coefficient, n. In the cases where the Hill coefficient was near 1, the K_{app} was recalculated using Eq. 2. The results are plotted in Fig. 3. Fig. 3 *A* compares the ionic strength dependence of the dissociation constant in the absence and presence of proadifen. At low ionic strength, the K_{app} values are similar in the absence or presence of proadifen. However, as the NaCl concentration increases, the K_{app} values diverge until the difference approaches that normally observed at physiological ionic strength.

In the presence of proadifen the corresponding Hill coefficients (n) shown in Fig. 3 *B* are close to 1, and display no ionic strength dependence. The titration binding data in the presence of proadifen at any ionic strength were well-fit with the simple binding equation, showing no cooperativity. Likewise, in the absence of proadifen at low ionic strength, n reduces to 1 (Fig. 3 *B*). However, in the absence of proadifen at high ionic strengths the binding data were best-fit with the Hill equation, and the Hill coefficient approached 1.6. The predominant change in affinity occurred in the range of 0–200 mM NaCl.

To determine the ionic strength dependence of the binding affinity in more detail we needed more data points than could be obtained reasonably by carrying out full binding isotherms at each ionic strength. Therefore, we chose to examine many NaCl concentrations at a single concentration of AChR and of Dns-C6-Cho. Fig. 4 *A* displays the fluorescence intensity of the specific bound Dns-C6-Cho in a suspension of 5 nm ACh binding sites and 6 nM Dns-C6-Cho as a function of ionic strength of the solution, in the absence (●) and presence (○) of proadifen. Using a calibration curve generated in the same experiment, the actual concentration of bound Dns-C6-Cho was determined from the observed fluorescence intensity. By obtaining the bound concentration of Dns-C6-Cho in this manner, the K_{app} at each NaCl concentration was calculated using Eq. 3, as described in Materials and Methods. The corresponding dissociation constants are displayed in Fig. 4 *B*. The results are consistent with those obtained from the binding isotherms (Fig. 3 *A*); in both cases the binding decreased with increasing ionic strength with smaller changes in the presence of proadifen. The largest changes in each curve occurred at NaCl concentrations $<$100 mM.

Group IA cations inhibit agonist binding

To test whether the effect of NaCl concentration on the binding affinity was due to specific interactions between

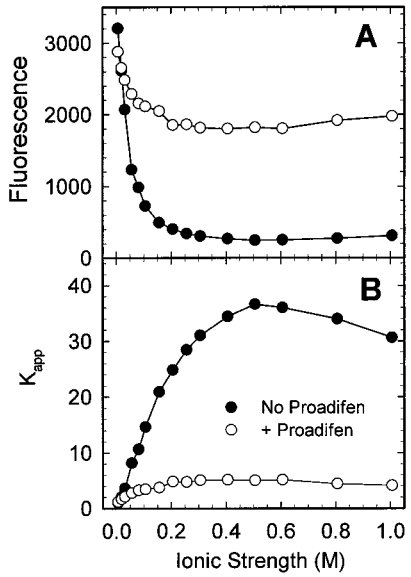

FIGURE 4 The ionic strength dependence of Dns-C6-Cho binding. (*A*) AChR-rich membranes (5 nM ACh sites) were incubated with 6 nM Dns-C6-Cho, with (○) or without (●) proadifen (10 μM), and with various concentrations of NaCl in 20 mM Hepes (pH 7.0) to give the indicated ionic strength. After 1 h equilibration, Dns-C6-Cho fluorescence was measured as described in Materials and Methods. Specific fluorescence was plotted from the difference in the presence and absence of 1 mM Carb. (*B*) K_{app} values without proadifen (●) and with proadifen (○), as calculated from the data in (*A*). To determine the concentration of bound Dns-C6-Cho from the fluorescence data, the proportionality constant for bound fluorescence, *C*, was determined by titration of Dns-C6-Cho into excess AChR (see Materials and Methods). From the value of bound Dns-C6-Cho concentration, the known concentrations of ACh binding sites, and the added Dns-C6-Cho, the K_{app} for binding was calculated for each ionic strength using Eq. 3.

Na^+ and the receptor or due to nonspecific electrostatic effects, salts other than NaCl were also used to control the ionic strength. Fig. 5 *A* shows the results using salts of the group IA monovalent cations: LiCl, NaCl, KCl, RbCl, and CsCl. All the monovalent cations tested reduce the binding of Dns-C6-Cho similarly, but reach distinct levels of binding at higher ionic strengths. The corresponding binding data carried out in 10 μM proadifen are shown in Fig. 5 *B*. The binding was likewise reduced by increasing salt concentrations, and the various ions differed in the extent of inhibition observed. Except for Cs^+, the binding data tend toward minimum plateau values at concentrations of salt up to 1 M (data not shown; the range in Fig. 5 goes only to 0.25 M). Nonetheless, the cations in Fig. 5 clearly display ion-specific effects on the affinity. The rank order of the extent of inhibition of binding (Fig. 5 *A*) is the same as the periodic table, and therefore correlates with the cation size or, inversely, with dehydration energy.

[^{3}H]Ethidium binding

The data shown above clearly reveal ionic effects on agonist affinity and that increased ionic strength facilitates proadifen effects on agonist affinity. These changes, therefore, suggest that ionic strength affects the conformational equilibrium of the AChR. A second method to test this notion is to examine the reciprocal effect of agonist upon the binding of the desensitizing NCA, EB. EB is suitable for this measurement because it is strongly sensitive to desensitization and affinity can be measured by radioligand binding (Herz et al., 1987; Lurtz et al., 1997; Pedersen, 1995). EB binding was examined at various ionic strengths in the presence and absence of the agonist Carb. Fig. 6 *A* shows the ratio of specifically bound [^{3}H]EB to free [^{3}H]EB, a value that is proportional to the affinity under these conditions, as a function of ionic strength, while the receptor and total EB concentrations were kept fixed. The dissociation constants for EB were calculated using Eq. 4 (Fig. 6 *B*). Compare this figure with Figs. 3 *A* and 4 *B*: there exists remarkable similarity between the binding of Dns-C6-Cho to the ACh site and the binding of [^{3}H]EB to the channel site. The dissociation constant in both cases increases with ionic strength. At high ionic strengths the dissociation constants in the absence of a desensitizing ligand were much higher

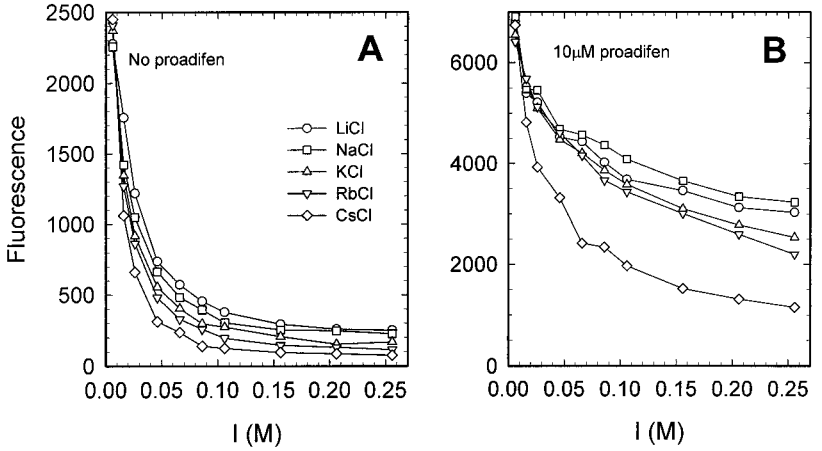

FIGURE 5 Monovalent ions affect Dns-C6-Cho binding similarly. Dns-C6-Cho binding to the ACh sites was determined in varying concentrations of the group IA chloride salts. AChR-rich membranes (5 nM ACh sites) were incubated with Dns-C6-Cho (6 nM) and the indicated concentration of the salts (○, CsCl; □, RbCl; △, KCl; ▽, NaCl; ◇, LiCl) in 20 mM Hepes (pH 7.0) for 1 h. Fluorescence intensity was then measured as described in Materials and Methods, in the presence and absence of 1 mM Carb; the specific fluorescence was determined from the difference. (*A*) No proadifen; (*B*) 10 μM proadifen.

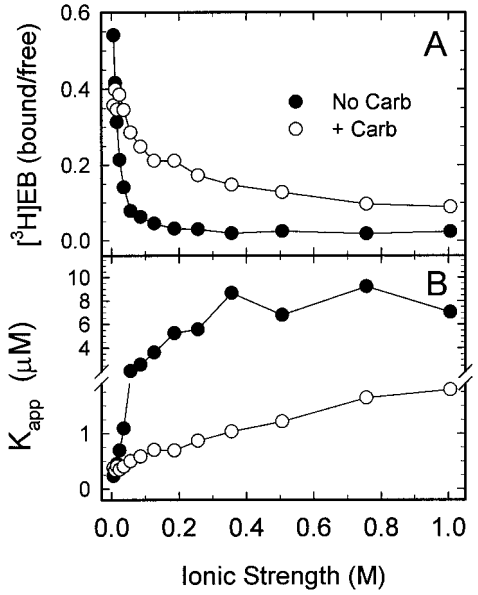

FIGURE 6 The ionic strength dependence of ethidium binding to the noncompetitive antagonist site of the AChR. AChR-rich membranes (100 μg; 337 nM ACh sites) were incubated with [^{3}H]EB (34 nM), with (○) or without (●) Carb (1 mM), and indicated concentration of NaCl in 20 mM Hepes (pH 7.0) for 1 h. Bound and free [^{3}H]EB were then determined after separation by centrifugation as described in Materials and Methods. The data were corrected for nonspecific binding by including 0.5 mM PCP. (*A*) The ratio of bound/free [^{3}H]EB; (*B*) the dissociation constants in the absence and presence of Carb calculated from the data in (*A*) according to Eq. 4.

than that in its presence. In both cases the K_{app} values converge at low ionic strength.

The dependence of the allosteric constant *M* on ionic strength

The conformational equilibrium of the AChR is described by the ratio of concentrations of desensitized to resting receptor ($M = [D]/[R]$; see Schemes I and II). This allosteric constant, M, can be estimated from the change in K_{app} caused by addition of an allosteric desensitizing ligand using Eq. 11, given in Materials and Methods.

The allosteric constant was calculated as a function of ionic strength from the Dns-C6-Cho binding data shown in Figs. 3 *A* and 4 *B*, and from the EB binding data shown in Fig. 6. For the Dns-C6-Cho binding data M was calculated assuming either the one site model (Scheme I; Fig. 7 *A*, *circles*) or the two-site model (Scheme II; Fig. 7 *A*, *squares*). The two-site model yields substantially lower values for M. The values determined by EB binding agree with those determined by calculating M from the single-site model for Dns-C6-Cho binding. The M value increases 30–100-fold as ionic strength is decreased, but it is unclear whether the upper limit of M has been reached at the lowest ionic strengths tested.

The EB and Dns-C6-Cho calculations in Fig. 7 *A* were derived from data obtained by varying the NaCl concentration. Because other monovalent cations affect binding to various extents (Fig. 5), we also determined the value for M in each of the group IA cations at a single high ionic strength (250 mM). Binding isotherms were carried out in buffer with each of the salts, in the presence and absence of proadifen, and the value of M calculated according to Eq. 11, corresponding to Scheme I. As shown in Fig. 7 *B*, the resultant values were similar; this demonstrates that the value of M does not depend on the type of monovalent cation used. This result further suggests that the distinct effects of salts on the extent of binding shown in Fig. 5 were due to differential effects of salts on the binding of Dns-C6-Cho itself rather than effects on the conformational equilibrium.

An alternative method for measuring desensitized AChR is by determining the percentage of AChR that initially binds agonist with high affinity, before the slow onset of agonist-induced desensitization (Boyd and Cohen, 1980). In preliminary experiments we examined the binding kinetics of Dns-C6-Cho using stopped-flow fluorescence, and found that in the physiological buffer HTPS ~20% of the receptor was in a high-affinity state before the onset of slow, Dns-C6-Cho-induced desensitization (data not shown). This corresponds to a value for M of 0.25. Parallel experiments carried out in the presence of proadifen were consistent with desensitization of >90% of the AChR, corresponding to an M value of >10. These data reflect a somewhat more direct method for determining M and yield values consistent with those obtained from the EB binding data and from analysis of the Dns-C6-Cho binding data as analyzed with the single binding site model (Scheme I and Eq. 11).

The change in M is 25–30 fold, as estimated from calculations of EB binding and the Dns-C6-Cho binding data from the single-site model. When the two-site model is used, the change in M approaches 100-fold. The 30- to 100-fold change in the allosteric constant represents a significant change in the conformational equilibrium.

DISCUSSION AND CONCLUSIONS

The data presented above demonstrate that increasing ionic strength lowers the affinity of agonists for the ACh binding sites of the AChR, and further show that the change is *smaller* in the presence of the desensitizing noncompetitive antagonist, proadifen. The effect of salt on affinity, therefore, had two distinct components: a direct effect on the binding affinity of agonists and a second effect mediated by altering the conformational equilibrium between the desensitized and resting states. At low ionic strength, cooperativity of agonist binding is lost and the ability of proadifen to influence agonist affinity is lost. The observations are consistent with preferential stabilization of the high-affinity, desensitized conformation of the AChR at low ionic

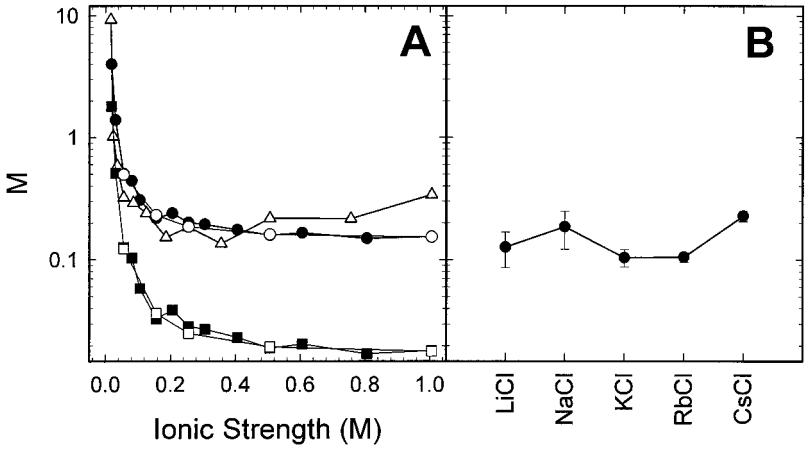

FIGURE 7 The ionic strength dependence of the allosteric constant (M). (A) The value of M was calculated from Dns-C6-Cho binding data shown in Fig. 4 B (●, ■) and the summarized data from binding isotherms shown in Fig. 3 A (○, □). M was calculated using either the single-binding site model, Eq. 11 (○, ●), or the two-binding site model, Eq. 12 (□, ■), as described in Materials and Methods. M was also calculated from [^{3}H]EB binding data (Fig. 6 A) using Eq. 11 (△). (B) The M of monovalent salts at physiological ionic strength (●). AChR (5 nM ACh sites) in 10 mM Hepes/250 mM salt was titrated with concentrated Dns-C6-Cho as described in Materials and Methods. K_D and K_{app} values were determined from binding isotherms measured in the presence and absence of 10 μM proadifen, respectively. M was then calculated for the indicated salts from K_D and K_{app} values using Eq. 11. Nonspecific binding was determined from parallel titrations that included 1 mM Carb.

strength. Below, we discuss separately these two effects of ionic strength changes on affinity.

Desensitization of AChR at low ionic strength

The extent of desensitization at various ionic strengths, expressed by the equilibrium constant, M, was calculated from the Dns-C6-Cho binding data (Fig. 7) using Eq. 12, which corresponds to the two-binding-site model (Scheme II). However, it is unclear why these low M values differ substantially from those observed by EB binding. The M values determined from EB binding data agree with our estimates of the desensitized population from rapid kinetic measurements of pre-existing, high-affinity AChR (data not shown), with published values for the extent of desensitization (Boyd and Cohen, 1984), and with a recent characterization of Dns-C6-Cho binding (Raines and Krishnan, 1998, $M = 0.1$). Perhaps coincidentally, when the Dns-C6-Cho binding data were analyzed by the single-site binding scheme (I), it yielded values consistent with the EB binding data. The primary assumption made in these calculations was that the microscopic binding constants for the resting state conformation (K_R) be significantly higher than the observed binding constants (K_{app}). This was true for Dns-C6-Cho, where the lower K of the two binding steps to the resting state (K_{R1}) was estimated at 1 μM (Raines and Krishnan, 1998), a value >20-fold higher than the highest K_{app} we observed, and therefore not a significant source of error in the calculation. We also considered models with assumptions of widely differing K_R values at each site (from our measurements, the K_D values are the same at each site) or with varying fluorescence yield at each site. These more elaborate two-site models yielded M values consistent with the simple two-site model. Understanding the source of this discrepancy in M will, therefore, require further experimentation.

Despite the model-dependent discrepancy in the absolute values of M, the results from both schemes indicate that the receptor is relatively more desensitized at low ionic strength and the resting-state population increases as ionic strength increases. The measured change in M (30–100-fold) reflects a minimum estimate because the lowest ionic strength tested was 6 mM. These changes correspond to free energy changes of 2 to 2.7 kcal/mol. Regardless of the model used, this represents a significant shift of the conformational equilibrium with ionic strength.

Various monovalent salts were tested for their effects on affinity and the extent of desensitization was determined using Eq. 10. It was found that desensitization was essentially independent of the type of cation used (Fig. 7 B). This suggests that the change in conformation induced by ionic strength changes was due not to ion binding interactions, but rather to electrostatic screening. That observation further suggests that the effects can be interpreted in terms of simple electrostatic repulsion or attraction.

A structural model for desensitization

The electrostatic screening that drives the conformational change with ionic strength must be due to interactions of surface charges with intervening solvent. If the charges were buried or separated only by protein, the charge interactions would not be expected to be moderated by ionic strength changes. Interaction among charged surface resi-

dues will be subject to electrostatic shielding by solvent ions at higher ionic strengths that will diminish electrostatic attraction between opposite charges and repulsion between like charges. It is of interest to consider the possible loci for charges that would move relatively to each other during the conformational change. In principle, such charged groups can reside anywhere on the conformational pathway involved in desensitization, but two likely options are residues near the ACh binding sites and residues in the pore. These two regions are known to undergo structural changes that cause changes in affinity for agonists and antagonists.

Structural models by Furois-Corbin and Pullman (1989) of the M2 helix in the pore indicate a concerted separation of the outer ring of negative charges (Imoto et al., 1988) upon desensitization. This model was supported by the labeling pattern of 3-trifluoromethyl-3-(*m*-[^{125}I]iodophenyl) diazirine (White and Cohen, 1992). This charge separation should be stabilized by decreased ionic screening at low ionic strength, a prediction that is consistent with our observations (Fig. 8). Alternatively, at the ACh binding sites, several residues have been identified that may be involved in charge-dependent conformational changes. Mutation of residue γLys-34 affects agonist binding (Prince and Sine, 1996; Sine et al., 1995); however, in the presence of proadifen, which desensitizes the AChR, the effect of mutation on binding was modest. Mutation of γAsp-174 or the homologous δ subunit amino acid, δAsp-180, has larger effects on agonist affinity than on *d*-tubocurarine binding (Martin et al., 1996). Because *d*-tubocurarine desensitizes substantially less than agonists (Pedersen and Papineni, 1995), this observation is consistent with effects on the conformational equilibrium rather than a direct interaction with the ligand charge. Electrostatic interactions of these residues with other nearby charges could result in the ionic strength effects on conformational change that we observed. These hypotheses can be tested by measuring *M* for AChRs mutagenized at candidate residues.

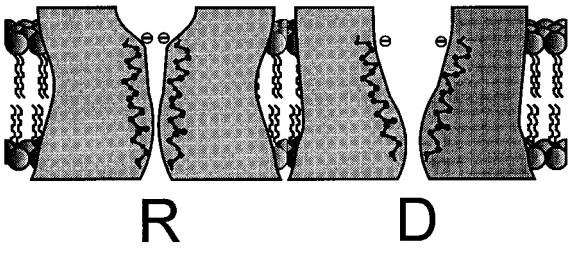

FIGURE 8 A model for charge-rearrangement upon desensitization of the AChR. Two cross-sectional views of the transmembrane region of the AChR are shown with distinct placement of the M2 putative transmembrane α-helices that correspond to the resting and desensitized conformations of the AChR.

Negative charges at the ACh binding sites

In addition to modulation of the conformational equilibrium, ions clearly affect binding through local effects at or near the binding site itself. These were seen most clearly when conformational equilibria were suppressed by maintaining the AChR in the desensitized conformation in the presence of proadifen. Addition of NaCl decreased binding until concentrations of 200 mM, whereupon no further loss of binding was observed (Figs. 4 and 5). This is inconsistent with inhibition through a purely competitive mechanism where Na^+ binds to a site and sterically blocks the ACh binding site, as illustrated in Fig. 9 *A*. Similar patterns of inhibition were observed for Li^+, K^+, and Rb^+, indicating that they also do not directly compete for binding. In contrast, from electrophysiological measurements of association rates of ACh for the mouse AChR, Akk and Auerbach (1996) concluded that Na^+, K^+, and Cs^+ bind directly to the ACh binding sites. However, their observations tested cations over a modest concentration range that may not have excluded allosteric or other mechanisms. Our data preclude direct, competitive binding of Na^+ and K^+ to the *Torpedo* AChR, though not necessarily for Cs^+.

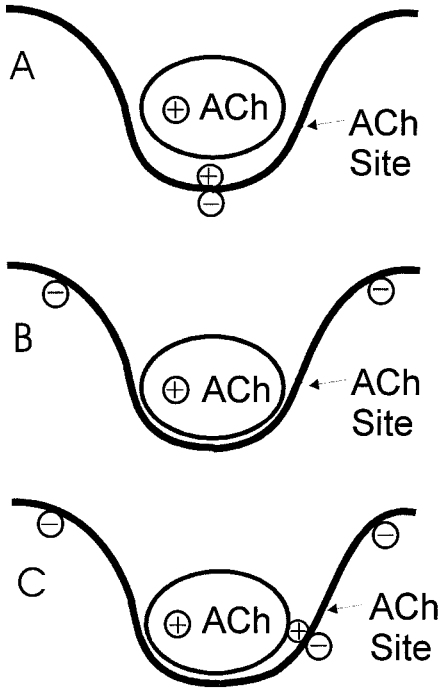

FIGURE 9 Models for inhibition of ACh binding by cations. (*A*) Competitive model; a negative site is located at the ACh site and binding of a cation directly blocks the binding of agonist. (*B*) Pure electrostatic model; negative charges are dispersed near the ACh site. Debye-Hückel-type electrostatic screening of these charges results in decreased agonist affinity. (*C*) Electrostatic plus steric interaction model: same as (*B*) with a charge located at the edge of the ACh site, forming a negative subsite. Large cations bind to the subsite, sterically destabilizing agonist binding to an extent that depends on cation size.

The noncompetitive nature of the cation effect on agonist binding suggests that electrostatic screening of charges near the ACh site was responsible for the change in agonist binding affinities. However, different cations affected binding to different extents: clearly, there exists some cation specificity. Thus, a model of pure Debye-Hückel-type electrostatic screening of charges near the ACh site cannot account for the effects of all the ions tested (illustrated in Fig. 9 *B*).

One possible explanation for cation specificity is that a negative subsite exists at the edge of the ACh binding site, as illustrated in Fig. 9 *C*. Such a subsite would be close enough to the bound agonist so that a bound cation will interact with the agonist sterically, but without blocking binding altogether. According to this model, larger cations would generate greater destabilization. Thus, the rank order of the extent of decrease in agonist binding affinity would correlate with cation size, as we observed.

The effects of the smaller cations, Li^+, Na^+, and K^+, on agonist affinity were similar, suggesting that purely ionic screening effects dominate the effects of small ions, rather than the steric effect from the negative subsite, which appears more important for Rb^+ and Cs^+. If we interpret the effects of small cations in terms of purely electrostatic screening, then Debye-Hückel theory (Eq. 8) may be applied to extract values for the effective charge distribution near the agonist binding sites. The ionic strength dependence of the dissociation constant of the desensitized conformation, as defined by the presence of proadifen, was fit to Eq. 8, and the result is displayed in Fig. 10. The best fit of the data obtained from binding isotherms (○, *dotted line*), at ionic strengths ≤0.5 M) gives the following values: $z_R = -8.1$, $r = 1.9$ nm, and $K_0 = 0.48$ nM for the effective charge at the binding site, the effective radius, and the dissociation constant at zero ionic strength, respectively. From fitting the data of single-concentration measurements (●, *solid line*), $z_R = -8.8$, $r = 2.0$ nm, and $K_0 = 0.39$ nM.

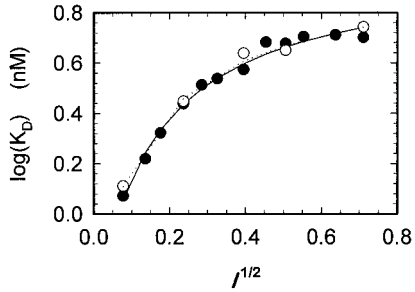

FIGURE 10 The charge distribution at the Dns-C6-Cho binding site. The dependence of the log of the dissociation constants for Dns-C6-Cho binding, in the presence of proadifen, on the square root of the ionic strength ($I^{1/2}$) were fitted with the Eq. 8. The *solid curve* represents the best fit of K_D values from Fig. 3 (○) as determined from binding isotherms. The dotted line is the best fit to K_D values from measurements at single Dns-C6-Cho concentrations from Fig. 4 (●).

Because Debye-Hückel theory is generally only valid for dilute solutions, we also examined the data at ionic strength <0.1 M, and obtained $Z_R = -5.1$, $r = 1.0$ nm, and $K_0 = 0.56$ nM. Thus, about five to nine net negative charges with an effective radius of 1 to 2 nm are distributed at or near the ACh sites.

Stauffer and Karlin (1994) estimated two to three charges at the ACh sites by measuring the rate of reaction of variously charged methanethiosulfonates with αCys-192/193. The difference between their conclusion and ours may reflect the distinct techniques used or that the vicinity of αCys-192/193 may differ from that of the binding site per se. The methods we used for this analysis were similar to those used by Nolte et al. (1980) to analyze the charge distribution near the active site of acetylcholinesterase. They found an effective charge of −6 to −9 that they predicted were distributed in a broad area on the surface of the protein. Nonetheless, their results were often interpreted as evidence for a cluster of charges in close apposition to ACh, acting as a countercharge or salt bridge (Quinn, 1987). Later, the x-ray crystal structure showed the presence of only one negative group in the active site and many negatively charged groups dispersed over a large surface area (Sussman et al., 1991). Likewise, our analysis is consistent with a model of multiple negative charges dispersed near the ACh binding site.

CONCLUSIONS

The AChR was found to be substantially desensitized at low ionic strength. The fraction of desensitized AChR, which is ~10–20% at high ionic strength, increases as the ionic strength decreases through effects likely mediated by electrostatic screening of charged residues that move relative to each other during the conformational transition. Five to nine negatively charged groups exist at or near the ACh sites in the extracellular domains. The interactions between small cations and the ACh sites are noncompetitive, whereas larger ions may contribute to inhibition by direct binding near the site.

This work was supported by United States Public Health Service Grant NS35212 and by Grant Q1406 from the Robert A. Welch Foundation. Xing-Zhi Song was supported by National Institutes of Health training grants HL07676 (institutional) and GM19672 (individual).

REFERENCES

Addona, G. H., S. H. Andrews, and D. S. Cafiso. 1997. Estimating the electrostatic potential at the acetylcholine receptor agonist site using power saturation EPR. *Biochim. Biophys. Acta.* 1329:74–84.

Akk, G., and A. Auerbach. 1996. Inorganic, monovalent cations compete with agonists for the transmitter binding site of nicotinic acetylcholine receptors. *Biophys. J.* 70:2652–2658.

Barrantes, F. J. 1998. The Nicotinic Acetylcholine Receptor: Current Views and Future Trends. Springer-Verlag, Berlin.

Blount, P., and J. P. Merlie. 1989. Molecular basis of the two nonequivalent ligand binding sites of the muscle nicotinic acetylcholine receptor. *Neuron.* 3:349–357.

Boyd, N. D., and J. B. Cohen. 1980. Kinetics of binding of [^{3}H]acetylcholine to *Torpedo* postsynaptic membranes: association and dissociation rate constants by rapid mixing and ultrafiltration. *Biochemistry.* 19: 5353–5358.

Boyd, N. D., and J. B. Cohen. 1984. Desensitization of membrane-bound *Torpedo* acetylcholine receptor by amine noncompetitive antagonists and aliphatic alcohols: studies of [^{3}H]acetylcholine binding and $^{22}Na^+$ ion fluxes. *Biochemistry.* 23:4023–4033.

Changeux, J. P., A. Devillers-Thiery, and P. Chemouilli. 1984. Acetylcholine receptor: an allosteric protein. *Science.* 225:1335–1345.

Cohen, J. B., L. A. Correll, E. B. Dreyer, I. R. Kuisk, D. C. Medynski, and N. P. Strnad. 1986. Interactions of local anesthetics with *Torpedo* nicotinic acetylcholine receptors. *In* Molecular and Cellular Mechanisms of Anesthetics. Plenum Publishing Corporation, New York. 111–124.

Czajkowski, C., and A. Karlin. 1995. Structure of the nicotinic receptor acetylcholine-binding site. Identification of acidic residues in the delta subunit within 0.9 nm of the alpha subunit-binding site disulfide. *J. Biol. Chem.* 270:3160–3164.

Devillers-Thiery, A., J. L. Galzi, J. L. Eisele, S. Bertrand, and J.-P. Changeux. 1993. Functional architecture of the nicotinic acetylcholine receptor: a prototype of ligand-gated ion channels. *J. Membr. Biol.* 136:97–112.

Dougherty, D. A. 1996. Cation-pi interactions in chemistry and biology: a new view of benzene, Phe, Tyr, and Trp. *Science.* 271:163–168.

Furois-Corbin, S., and A. Pullman. 1989. A possible model for the inner wall of the acetylcholine receptor channel. *Biochim. Biophys. Acta.* 984:339–350.

Heidmann, T., J. Bernhardt, E. Neumann, and J. P. Changeux. 1983. Rapid kinetics of agonist binding and permeability response analyzed in parallel on acetylcholine receptor rich membranes from *Torpedo marmorata. Biochemistry.* 22:5452–5459.

Herz, J. M., D. A. Johnson, and P. Taylor. 1987. Interaction of noncompetitive inhibitors with the acetylcholine receptor. The site specificity and spectroscopic properties of ethidium binding. *J. Biol. Chem.* 262:7238–7247.

Hucho, F., V. I. Tsetlin, and J. Machold. 1996. The emerging three-dimensional structure of a receptor. The nicotinic acetylcholine receptor. *Eur. J. Biochem.* 239:539–557.

Imoto, K., C. Busch, B. Sakmann, M. Mishina, T. Konno, J. Nakai, H. Bujo, Y. Mori, K. Fukuda, and S. Numa. 1988. Rings of negatively charged amino acids determine the acetylcholine receptor channel conductance. *Nature.* 335:645–648.

Katz, B., and S. Thesleff. 1957. A study of the desensitization produced by acetylcholine at the motor endplate. *J. Physiol.* 138:63–80.

Krodel, E. K., R. A. Beckman, and J. B. Cohen. 1979. Identification of a local anesthetic binding site in nicotinic post-synaptic membranes isolated from *Torpedo marmorata* electric tissue. *Mol. Pharmacol.* 15:294–312.

Levine, I. 1988. Physical Chemistry. McGraw-Hill Book Company, New York.

Lurtz, M. M., M. L. Hareland, and S. E. Pedersen. 1997. Quinacrine and ethidium bromide bind the same locus on the nicotinic acetylcholine receptor from *Torpedo californica. Biochemistry.* 36:2068–2075.

Martin, M., C. Czajkowski, and A. Karlin. 1996. The contributions of aspartyl residues in the acetylcholine receptor gamma and delta subunits to the binding of agonists and competitive antagonists. *J. Biol. Chem.* 271:13497–13503.

Neher, E., and J. H. Steinbach. 1978. Local anaesthetics transiently block currents through single acetylcholine-receptor channels. *J. Physiol.* 277: 153–176.

Neubig, R. R., and J. B. Cohen. 1979. Equilibrium binding of [^{3}H]tubocurarine and [^{3}H]acetylcholine by *Torpedo* postsynaptic membranes: stoichiometry and ligand interactions. *Biochemistry.* 18:5464–5475.

Nolte, H. J., T. L. Rosenberry, and E. Neumann. 1980. Effective charge on acetylcholinesterase active sites determined from the ionic strength dependence of association rate constants with cationic ligands. *Biochemistry.* 19:3705–3711.

Ochoa, E. L., A. Chattopadhyay, and M. G. McNamee. 1989. Desensitization of the nicotinic acetylcholine receptor: molecular mechanisms and effect of modulators. *Cell Mol. Neurobiol.* 9:141–178.

Pedersen, S. E. 1995. Site-selective photoaffinity labeling of the *Torpedo californica* nicotinic acetylcholine receptor by azide derivatives of ethidium bromide. *Mol. Pharmacol.* 47:1–9.

Pedersen, S. E., and J. B. Cohen. 1990. d-Tubocurarine binding sites are located at alpha-gamma and alpha-delta subunit interfaces of the nicotinic acetylcholine receptor. *Proc. Natl. Acad. Sci. USA.* 87:2785–2789.

Pedersen, S. E., E. B. Dreyer, and J. B. Cohen. 1986. Location of ligand-binding sites on the nicotinic acetylcholine receptor alpha-subunit. *J. Biol. Chem.* 261:13735–13743.

Pedersen, S. E., and R. V. Papineni. 1995. Interaction of d-tubocurarine analogs with the *Torpedo* nicotinic acetylcholine receptor. Methylation and stereoisomerization affect site-selective competitive binding and binding to the noncompetitive site. *J. Biol. Chem.* 270:31141–31150.

Prince, R. J., and S. M. Sine. 1996. Molecular dissection of subunit interfaces in the acetylcholine receptor. Identification of residues that determine agonist selectivity. *J. Biol. Chem.* 271:25770–25777.

Quinn, D. M. 1987. Acetylcholinesterase: enzyme structure, reaction dynamics, and virtual transition states. *Chem. Rev.* 87:955–979.

Raines, D. E., and N. S. Krishnan. 1998. Transient low-affinity agonist binding to *Torpedo* postsynaptic membranes resolved by using sequential mixing stopped-flow fluorescence spectroscopy. *Biochemistry.* 37: 956–964.

Schmidt, J., and M. A. Raftery. 1974. The cation sensitivity of the acetylcholine receptor from *Torpedo californica. J. Neurochem.* 23:617–623.

Sine, S. M., T. Claudio, and F. J. Sigworth. 1990. Activation of *Torpedo* acetylcholine receptors expressed in mouse fibroblasts. Single channel current kinetics reveal distinct agonist binding affinities. *J. Gen. Phys.* 96:395–437.

Sine, S. M., H. J. Kreienkamp, N. Bren, R. Maeda, and P. Taylor. 1995. Molecular dissection of subunit interfaces in the acetylcholine receptor: identification of determinants of alpha-conotoxin M1 selectivity. *Neuron.* 15:205–211.

Sobel, A., M. Weber, and J.-P. Changeux. 1977. Large-scale purification of the acetylcholine-receptor protein in its membrane-bound and detergent extracted forms from *Torpedo marmorata* electric organ. *Eur. J. Biochem.* 80:215–224.

Stauffer, D. A., and A. Karlin. 1994. Electrostatic potential of the acetylcholine binding sites in the nicotinic receptor probed by reactions of binding-site cysteines with charged methanethiosulfonates. *Biochemistry.* 33:6840–6849.

Sugiyama, N., A. E. Boyd, and P. Taylor. 1996. Anionic residue in the alpha-subunit of the nicotinic acetylcholine receptor contributing to subunit assembly and ligand binding. *J. Biol. Chem.* 271:26575–26581.

Sussman, J. L., M. Harel, F. Frolow, C. Oefner, A. Goldman, L. Toker, and I. Silman. 1991. Atomic structure of acetylcholinesterase from *Torpedo californica*: a prototypic acetylcholine-binding protein. *Science.* 253: 872–879.

Tan, R. C., T. N. Truong, J. A. McCammon, and J. L. Sussman. 1993. Acetylcholinesterase: electrostatic steering increases the rate of ligand binding. *Biochemistry.* 32:401–403.

Waksman, G., M. C. Fournie-Zaluski, and B. Roques. 1976. Synthesis of fluorescent acyl-cholines with agonistic properties: pharmacological activity on Electrophorus electroplaque and interaction in vitro with *Torpedo* receptor-rich membrane fragments. *FEBS Lett.* 67:335–342.

Walker, J. W., K. Takeyasu, and M. G. McNamee. 1982. Activation and inactivation kinetics of *Torpedo californica* acetylcholine receptor in reconstituted membranes. *Biochemistry.* 21:5384–5389.

White, B. H., and J. B. Cohen. 1992. Agonist-induced changes in the structure of the acetylcholine receptor M2 regions revealed by photoincorporation of an uncharged nicotinic noncompetitive antagonist. *J. Biol. Chem.* 267:15770–15783.

Zhong, W., J. P. Gallivan, Y. Zhang, L. Li, H. A. Lester, and D. A. Dougherty. 1998. From ab initio quantum mechanics to molecular neurobiology: a cation-pi binding site in the nicotinic receptor. *Proc. Natl. Acad. Sci. USA.* 95:12088–12093.